Supplement of Biogeosciences, 14, 5015–5027, 2017
https://doi.org/10.5194/bg-14-5015-2017-supplement

Biogeosciences Open Access EGU

Supplement of

A mechanistic model of an upper bound on oceanic carbon export as a function of mixed layer depth and temperature

Z. Li and N. Cassar

Correspondence to: Zuchuan Li (zuchuan.li@duke.edu)

1. Derivation of first and second derivatives of $NCP(0, MLD)$

To explore how $NCP(0, MLD)$ varies with C, we calculate its first and second derivatives with respect to C. Based on equations (8-10):

$$\frac{dNCP(0,MLD)}{dC}$$

$$= \frac{d\left\{-N_m \times \mu_{max} \times \frac{ln\left(\frac{I_0 \times e^{-K_I \times MLD} + k_m^I}{I_0 + k_m^I}\right) \times C}{K_I}\right\}}{dC} - \frac{d\{r_{HR} \times C \times MLD\}}{dC}$$

$$= -N_m \times \mu_{max}$$

$$\times \frac{\left\{ln\left(\frac{I_0 \times e^{-K_I \times MLD} + k_m^I}{I_0 + k_m^I}\right) - C \times \frac{I_0 + k_m^I}{I_0 \times e^{-K_I \times MLD} + k_m^I} \times \frac{I_0 \times e^{-K_I \times MLD}}{I_0 + k_m^I} \times k_c \times MLD\right\} \times K_I - k_c \times C \times ln\left(\frac{I_0 \times e^{-K_I \times MLD} + k_m^I}{I_0 + k_m^I}\right)}{{K_I}^2}$$

$$- r_{HR} \times MLD$$

$$= -N_m \times \mu_{max} \times \frac{\{-K_I \times I_m(0,MLD) - C \times I_m(MLD) \times k_c \times MLD\} \times K_I + k_c \times C \times K_I \times I_m(0,MLD)}{{K_I}^2} - r_{HR} \times MLD$$

$$= N_m \times \mu_{max} \times \frac{K_I \times I_m(0,MLD) + k_c \times C \times I_m(MLD) \times MLD - k_c \times C \times I_m(0,MLD)}{K_I} - r_{HR} \times MLD$$

$$= N_m \times \mu_{max} \times \frac{K_I \times I_m(0,MLD) - k_c \times C \times I_m(0,MLD) + k_c \times C \times MLD \times I_m(MLD)}{K_I} - r_{HR} \times MLD$$

$$= N_m \times \mu_{max} \times \frac{K_I^w \times I_m(0,MLD) + k_c \times C \times MLD \times I_m(MLD)}{K_I^w + k_c \times C} - r_{HR} \times MLD \qquad (S1)$$

where $I_m(MLD) = \frac{I_0 \times e^{-K_I \times MLD}}{I_0 \times e^{-K_I \times MLD} + k_m^I}$.

Based on equation (S1), the second derivative of $NCP(0, MLD)$ in equation (8) with respect to C may be expressed as follows:

$$\frac{d^2NCP(0,MLD)}{dC^2} = N_m \times \mu_{max} \times \left\{\frac{dy}{dC} + \frac{dg}{dC}\right\} \qquad (S2)$$

where $y = \frac{K_I^w \times I_m(0,MLD)}{K_I} = -\frac{K_I^w \times ln\left(\frac{I_0 \times e^{-K_I \times MLD} + k_m^I}{I_0 + k_m^I}\right)}{{K_I}^2}$ and $g = \frac{k_c \times C \times MLD \times I_m(MLD)}{K_I}$.

$\frac{dy}{dC}$ and $\frac{dg}{dC}$ are derived as follows:

$$\frac{dy}{dC} = -K_I^w \times \frac{\frac{I_0 + k_m^I}{I_0 \times e^{-K_I \times MLD} + k_m^I} \times \frac{I_0 \times e^{-K_I \times MLD}}{I_0 + k_m^I} \times (-k_c \times MLD) \times {K_I}^2 - ln\left(\frac{I_0 \times e^{-K_I \times MLD} + k_m^I}{I_0 + k_m^I}\right) \times 2 \times K_I \times k_c}{{K_I}^4}$$

$$= -K_I^w \times \frac{-I_m(MLD) \times MLD \times {K_I}^2 + I_m(0, MLD) \times 2 \times {K_I}^2}{{K_I}^4} \times k_c$$

$$= K_I^w \times \frac{I_m(MLD) \times MLD - 2 \times I_m(0, MLD)}{{K_I}^2} \times k_c \qquad (S3)$$

$$\frac{dg}{dC}$$

$$= \frac{-k_c \times C \times MLD \times I_m(MLD) \times k_c + k_c \times MLD \times I_m(MLD) \times K_I}{{K_I}^2}$$

$$+ \frac{k_c \times C \times MLD \times \frac{I_0 \times e^{-K_I \times MLD} \times (-k_c \times MLD) \times \{I_0 \times e^{-K_I \times MLD} + k_m^I\} - I_0 \times e^{-K_I \times MLD} \times I_0 \times e^{-K_I \times MLD} \times (-k_c \times MLD)}{\{I_0 \times e^{-K_I \times MLD} + k_m^I\}^2} \times K_I}{{K_I}^2}$$

$$= \frac{k_c \times MLD \times I_m(MLD) \times K_I + k_c \times C \times MLD \times \frac{I_0 \times e^{-K_I \times MLD} \times (-k_c \times MLD) \times k_m^I}{\{I_0 \times e^{-K_I \times MLD} + k_m^I\}^2} \times K_I - {k_c}^2 \times C \times MLD \times I_m(MLD)}{{K_I}^2}$$

$$= \frac{k_c \times MLD \times I_m(MLD) \times K_I + k_c \times C \times MLD \times \frac{I_m(MLD)^2 \times (-k_c \times MLD) \times k_m^I}{I_0 \times e^{-K_I \times MLD}} \times K_I - {k_c}^2 \times C \times MLD \times I_m(MLD)}{{K_I}^2}$$

$$= \frac{MLD \times I_m(MLD) \times K_I + k_c \times C \times MLD \times \frac{-I_m(MLD)^2 \times MLD \times k_m^I}{I_0 \times e^{-K_I \times MLD}} \times K_I - k_c \times C \times MLD \times I_m(MLD)}{{K_I}^2} \times k_c$$

$$= \frac{MLD \times I_m(MLD) \times K_I - k_c \times C \times MLD \times I_m(MLD)}{{K_I}^2} \times k_c - \frac{k_c \times C \times MLD \times \frac{I_m(MLD)^2 \times MLD \times k_m^I}{I_0 \times e^{-K_I \times MLD}} \times K_I}{{K_I}^2} \times k_c$$

$$= \frac{MLD \times I_m(MLD) \times K_I^w}{{K_I}^2} \times k_c - \frac{MLD^2 \times C \times I_m(MLD)^2 \times k_m^I}{K_I \times I_0 \times e^{-K_I \times MLD}} \times {k_c}^2 \quad (S4)$$

Substituting equations (S3-S4) into equation (S2) yields:

$$\frac{d^2 NCP(0, MLD)}{dC^2}$$

$$= N_m \times \mu_{max} \times \left\{K_I^w \times \frac{I_m(MLD) \times MLD - 2 \times I_m(0, MLD)}{{K_I}^2} \times k_c + \frac{MLD \times I_m(MLD) \times K_I^w}{{K_I}^2} \times k_c - \frac{MLD^2 \times C \times I_m(MLD)^2 \times k_m^I}{K_I \times I_0 \times e^{-K_I \times MLD}} \times {k_c}^2\right\}$$

$$= N_m \times \frac{\mu_{max}}{K_I} \times k_c \times \left\{\frac{2 \times K_I^w}{K_I} \times \left(I_m(MLD) \times MLD - I_m(0, MLD)\right) - \frac{MLD^2 \times C \times I_m(MLD)^2 \times k_m^I}{I_0 \times e^{-K_I \times MLD}} \times k_c\right\} \qquad (S5)$$

2. NCP upper bound for shallow MLD

When $0 \le MLD < MLD_{C^*_{max}}$ and $MLD \to 0$, $1 - \exp(-K_I \times MLD)$ in equation (15) can be approximated using a second order of Taylor expansion:

$$1 - \exp(-K_I \times MLD) \approx K_I \times MLD - \frac{1}{2} \times (K_I \times MLD)^2 \qquad (S6)$$

From equation (S6), we may approximate equation (15):

$$NCP(0, MLD) = C \times MLD \times \left(-\frac{1}{2} \times K_I \times MLD \times \mu^* + \mu^* - r_{HR}\right) \qquad (S7)$$

where the first derivative of equation (S7) with respective to C is:

$$\frac{dNCP(0, MLD)}{dC} = MLD \times \left(-K_I^{nw} \times MLD \times \mu^* - \frac{1}{2} \times K_I^w \times MLD \times \mu^* + \mu^* - r_{HR}\right) \qquad (S8)$$

when $0 \le MLD < MLD_{C^*_{max}}$, K_I^{nw} should satisfy $K_I^{nw} \le k_c \times C^*_{max} < -\frac{1}{2} \times K_I^w + \frac{\mu^* - r_{HR}}{\mu^*} \times \frac{1}{MLD}$, and equation (S8) should be greater than 0. $NCP(0, MLD)$ thus increases with C in the range of $0 \le MLD < MLD_{C^*_{max}}$, with an upper bound obtained at C^*_{max}:

$$NCP^* = \mu^* \times C^*_{max} \times MLD \times \left(-\frac{1}{2} \times (k_c \times C^*_{max} + K_I^w) \times MLD + \frac{\mu^* - r_{HR}}{\mu^*}\right) \qquad (S9)$$

Over this range, Equation (S9) states that NCP^* increases with MLD, and as expected is nil when MLD equals 0.

3. An upper bound on export ratio

The export ratio ef (equation (24)) is written as follows:

$$ef = \frac{NCP(0, MLD)}{NPP(0, MLD)} = 1 - \frac{K_I \times MLD}{-ln\left(\frac{I_0 \times e^{-K_I \times MLD} + k_m^I}{I_0 + k_m^I}\right)} \times \frac{1}{N_m} \times \frac{r_{HR}}{\mu_{max}} \qquad (S10)$$

The first derivative of ef with respect to C is expressed as:

$$\frac{\partial ef}{\partial C} = -\left(1 - \frac{MLD \times I_m(MLD)}{I_m(0, MLD)}\right) \times \frac{1}{K_I} \times k_c \times (1 - ef) \qquad (S11)$$

According to the inequality in equation (13), $\frac{\partial ef}{\partial C}$ in equation (S11) must be less than zero. Therefore, ef maximizes when $C \to 0$ ($ef = 1 - \frac{1}{I_m(0)} \times \frac{1}{N_m} \times \frac{r_{HR}}{\mu_{max}}$). Considering that the minimum values for the terms $\frac{1}{N_m}$

and $\frac{1}{I_m(0)}$ are 1, ef is maximized in equation (S10) with $ef^* = 1 - \frac{r_{HR}}{\mu_{max}} = 1 - \alpha \times e^{(B_T - P_T)\times T}$, where α represents an constant, $B_T = 0.11$ and $P_T = 0.0633$ for the equation (5) of Cael and Follows (2016).

4. Dataset

To test the performance of our upper bound model, we compiled observations of net community production (Table S1) and carbon export in the world's oceans.

4.1 O_2/Ar Net Community Production

The O_2/Ar method estimates NCP through a mass balance of biological O_2 in the mixed layer. Because Ar and O_2 have similar temperature dependencies and solubilities (Craig and Hayward, 1987), the saturation state of their ratio can partition oxygen concentration due to physical ($[O_2]_{phys}$) and biological processes ($[O_2]_{\mathrm{biol}}$) (Cassar et al., 2011):

$$[\mathrm{O_2}]_{\mathrm{biol}} = [\mathrm{O_2}] - [\mathrm{O_2}]_{\mathrm{phys}} \approx [\mathrm{O_2}] - \frac{[\mathrm{Ar}]}{[\mathrm{Ar}]_{\mathrm{sat}}}[\mathrm{O_2}]_{\mathrm{sat}} = \frac{[\mathrm{Ar}]}{[\mathrm{Ar}]_{\mathrm{sat}}}[\mathrm{O_2}]_{\mathrm{sat}}\Delta(\mathrm{O_2/Ar}) \qquad (S12)$$

where $\Delta(\mathrm{O_2/Ar}) = \left[\frac{([\mathrm{O_2}]/[\mathrm{Ar}])}{([\mathrm{O_2}]/[\mathrm{Ar}])_{\mathrm{sat}}} - 1\right]$ is the biological O_2 supersatulation. When ignoring vertical mixing and lateral advection, we can write the mass balance for $[\mathrm{O_2}]_{\mathrm{biol}}$ in the mixed layer as follows (Cassar et al., 2011):

$$MLD\frac{d[O_2]_{biol}}{dt} = NCP - k_{\mathrm{O_2}}\frac{[\mathrm{Ar}]}{[\mathrm{Ar}]_{\mathrm{sat}}}[\mathrm{O_2}]_{\mathrm{sat}}\Delta(\mathrm{O_2/Ar}) \qquad (S13)$$

where $k_{\mathrm{O_2}}$ is the gas exchange velocity for O_2. At steady state (i.e., $\frac{d[O_2]_{biol}}{dt} = 0$), equation (S13) reduces to (Cassar et al., 2011; Reuer et al., 2007):

$$\mathrm{NCP} = k_{\mathrm{O_2}}[\mathrm{O_2}]_{\mathrm{sat}}\Delta(\mathrm{O_2/Ar}) \qquad (S14)$$

where $\frac{[\mathrm{Ar}]}{[\mathrm{Ar}]_{\mathrm{sat}}}$ in equation (S13) is assumed to equal 1, which introduces an error of up to a couple percent in NCP estimates under most conditions (Cassar et al., 2011; Eveleth et al., 2014).

To derive NCP using equation (S14), we calculate $k_{\mathrm{O_2}}$ using daily NCEP wind speeds, MLD, the parameterization of Wanninkhof (1992), and a weighting technique to account for wind speed history following (Reuer et al., 2007). Uncertainties and biases in O_2/Ar NCP estimates can be found in previous studies (Bender et al., 2011; Cassar et al., 2014; Jonsson et al., 2013).

Table S1. O_2/Ar measurements included in this study.

Citation	Cruise	Start date	End date	Location
(Reuer et al., 2007)	A0103	10/30/2001	12/10/2001	South of Australia
	SOFEXR	01/07/2002	02/12/2002	South of New Zealand
	SOFEXM	01/20/2002	02/24/2002	South of New Zealand
	NBP0305	10/28/2003	11/13/2003	South of New Zealand
	ANTXXI/2	11/18/2003	01/15/2004	South of South Africa
	NBP0305A	12/20/2003	12/29/2003	South of New Zealand
(Cassar et al., 2007)	AA2006	12/03/2005	02/09/2006	South of Australia
(Juranek et al., 2010)	AMT16	05/22/2005	06/28/2005	Atlantic
	AMT17	10/18/2005	11/25/2005	Atlantic
(Stanley et al., 2010)	EUC-Fe	07/19/2006	08/31/2006	Equatorial Pacific
(Tortell et al., 2011)	CORSACS II	11/03/2006	12/11/2006	South of New Zealand
(Cassar et al., 2011)	SAZ-SENSE	01/19/2007	02/19/2007	South of Australia
(Huang et al., 2012)	LMG0801	01/07/2008	01/29/2008	Drake Passage
(Hamme et al., 2012)	GASEX	03/02/2008	04/11/2008	South of Atlantic
(Martin et al., 2013)	LOHAFEX	01/26/2009	03/06/2009	South of Atlantic
(Shadwick et al., 2015)	AA1203	01/08/2012	02/10/2012	South of Australia
(Eveleth et al., 2016)	LMG1201	12/30/2011	02/07/2012	Drake Passage
	LMG1301	01/05/2013	02/03/2013	Drake Passage
	LMG1401	01/01/2014	02/01/2014	Drake Passage
(Huang et al., unpublished)	LMG0901	01/06/2009	02/01/2009	Drake Passage
	LMG1001	01/01/2010	02/07/2010	Drake Passage
	LMG1101	01/02/2011	02/06/2011	Drake Passage

4.2 Sediment trap and ^{234}Thorium POC export production

We also compared NCP^* to sediment-trap and ^{234}Th-derived POC export production estimates from the dataset recently compiled by Mouw et al. (2016). These observations were adjusted to reflect a flux at the base of the mixed layer using the Martin curve with $b = -0.86$ (Martin et al., 1987). Monthly climatological MLD were used.

4.3 Mixed layer depth

We derived MLD using Argo temperature-salinity profiling floats which were downloaded from http://www.usgodae.org/. As real-time data (after 2008) have not been thoroughly checked, we only used profiles with temperature, salinity, and pressure with a quality flag of '1' ('good data') or '2' ('probably good data'). To improve coverage, we also used the temperature and salinity profiles obtained by CTD casts in the World Ocean Database. These profiles were downloaded from the National Oceanographic Data Center (NODC) https://www.nodc.noaa.gov/access/index.html.

MLD is estimated as the depth at which the potential density (σ_θ) exceeds a near-surface reference value at 10 m depth by $\Delta\sigma_\theta = 0.03$ kg m^{-3} (de Boyer Montegut et al., 2004; Dong et al., 2008). Estimates were averaged to daily $5° \times 5°$ grids, from which monthly climatologies were calculated (Figure S1).

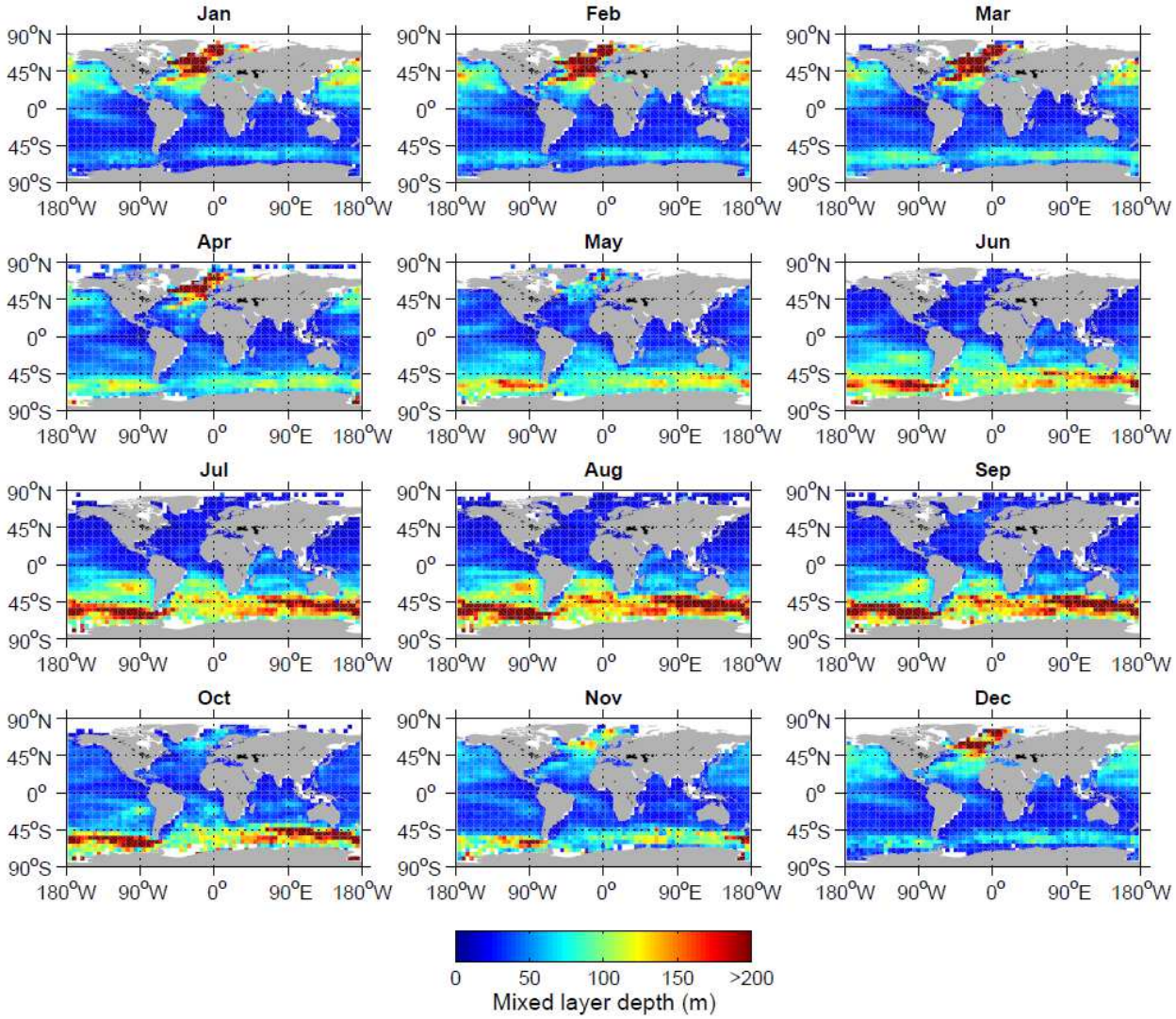

Figure S1. Climatology of monthly mixed layer depth.

4.4 Satellite properties

To derive a global distribution of NCP^*, we used monthly SST and PAR climatologies calculated based on MODIS-Aqua observations from 2002-2015 with a spatial resolution of $0.083° \times 0.083°$ (downloaded from NASA's ocean color website (http://oceancolor.gsfc.nasa.gov/cms/)). We compared $NCP^*$to monthly and annual NCP climatologies as simulated by the algorithms developed by Li and Cassar (2016). This NCP dataset represents the average of 11 satellite algorithms of export production for observations from 1997 to 2010 (Figure S2). More details can be found in Li and Cassar (2016).

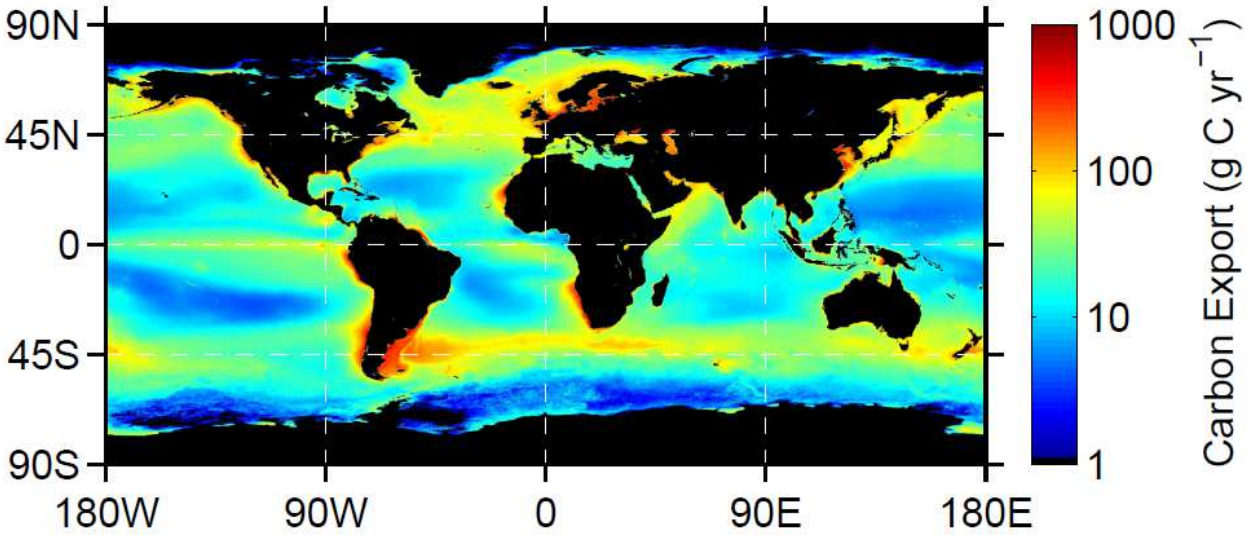

Figure 2S. Average annual export production derived using 11 algorithms (see Li and Cassar (2016)).

4.5. Diffusion attenuation coefficient for photosynthetically active radiation

Constants k_c and K_I^w in equation (10) were derived using the NOMAD dataset (Werdell and Bailey, 2005), which includes chlorophyll a concentration and K_I (Figure S3). NOMAD was downloaded from https://seabass.gsfc.nasa.gov/wiki/NOMAD. The regression in Figure S3 was converted to equation (10) using a carbon to chlorophyll ratio of 90 (Arrigo et al., 2008).

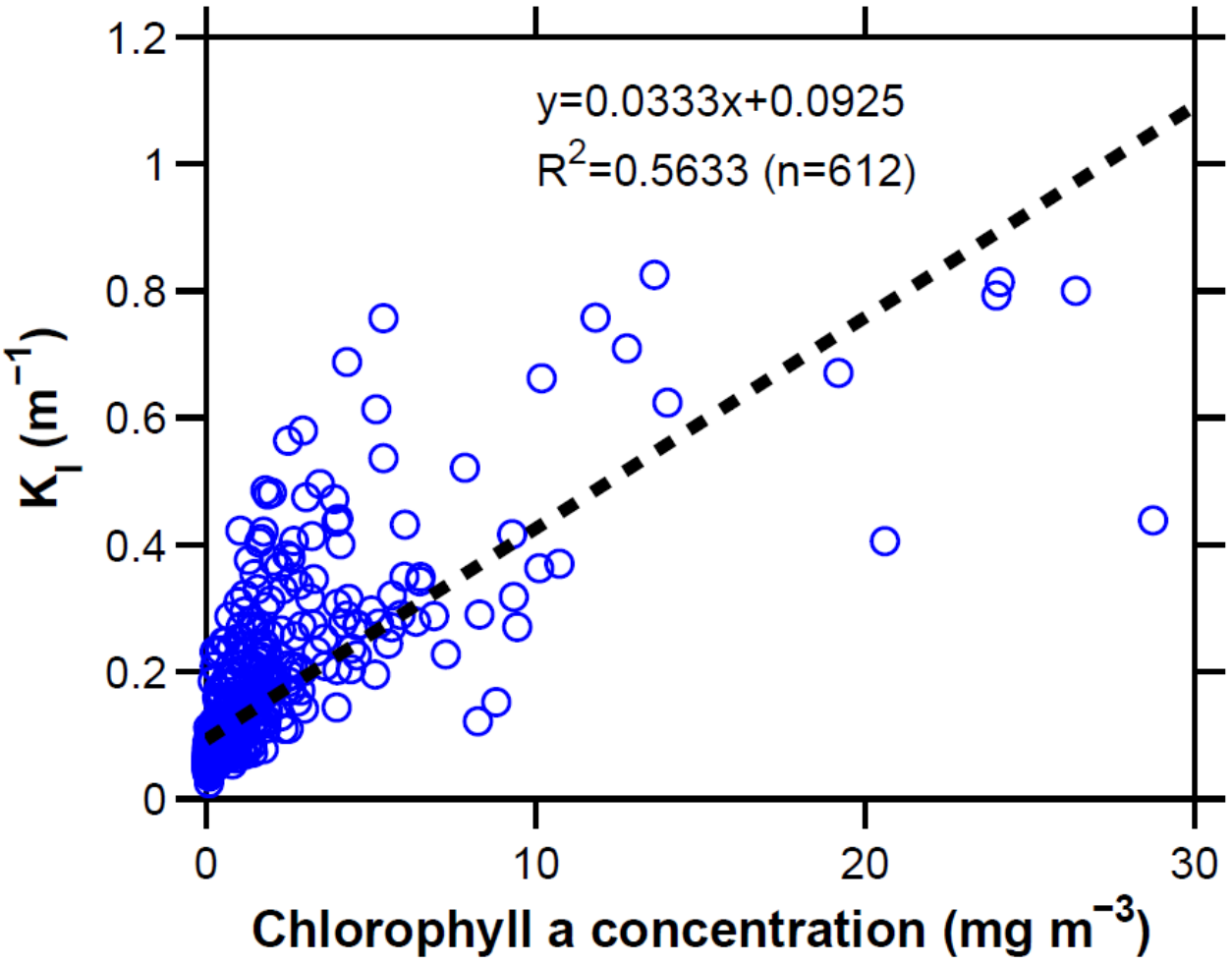

Figure S3. Attenuation coefficient for photosynthetically active radiation (PAR) as a function of chlorophyll a concentration based on the NOMAD dataset.

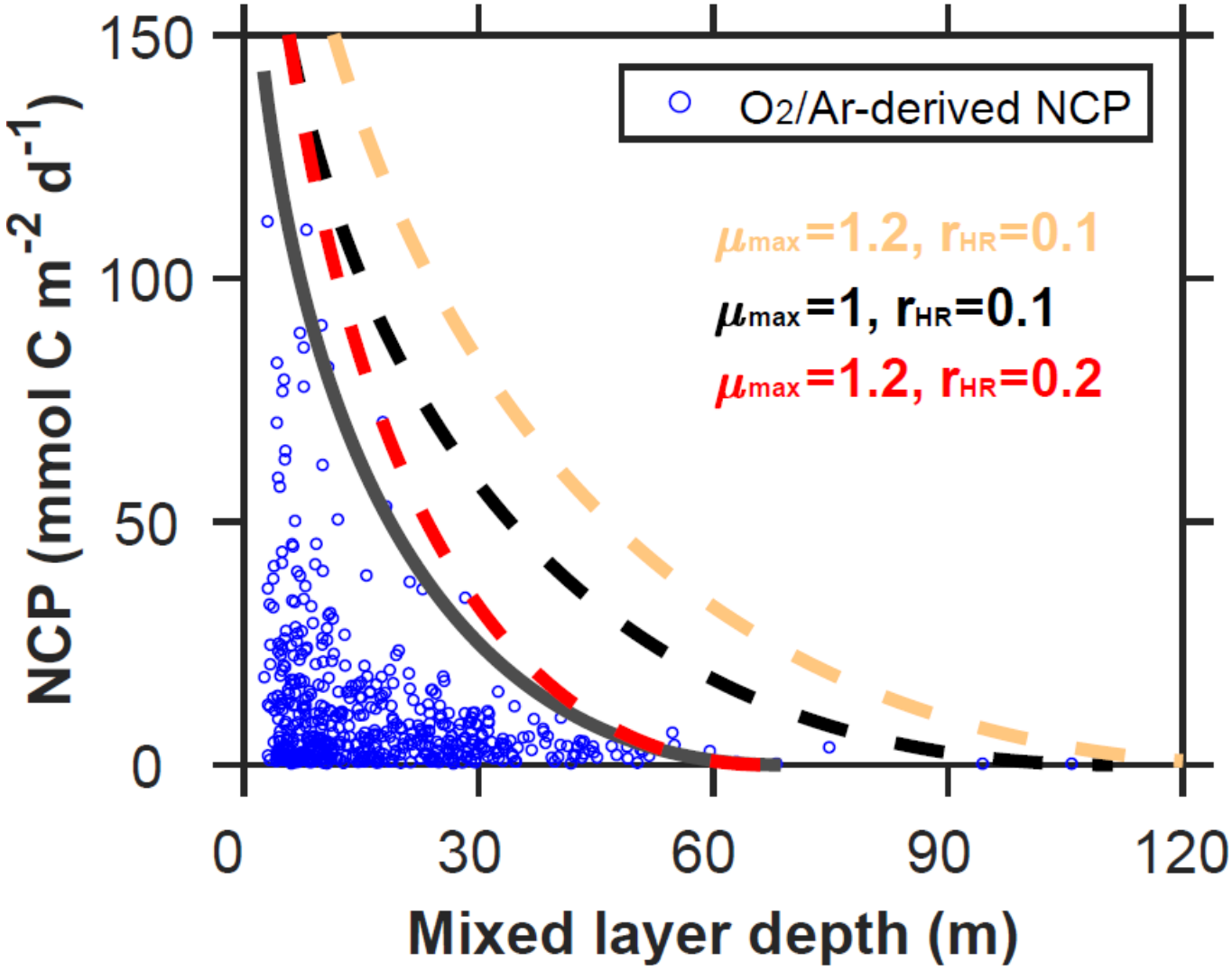

Figure S4. Modeled upper bound on carbon export production compared to field observations as a function of mixed layer depth (MLD). Observations are based on O_2/Ar-derived net community production (NCP). To account for the effect of photosynthetically active radiation (PAR) on export production, both MLD and carbon fluxes are normalized to $-log(1 - I_m(0))$ (see equations (19) and (21)). The thick gray line represents the upper bound fitted to the NCP data. Dash-lines represent the upper bounds calculated using parameters available in the literature (Table 2). A stoichiometric ratio of O_2/C=1.4 was used to convert NCP from O_2 to C units (Laws, 1991).

References

Arrigo, K. R., van Dijken, G. L., and Bushinsky, S.: Primary production in the Southern Ocean, 1997-2006, J. Geophys. Res., 113, doi:10.1029/2007JC004551, 2008.

Bender, M. L., Kinter, S., Cassar, N., and Wanninkhof, R.: Evaluating gas transfer velocity parameterizations using upper ocean radon distributions, J. Geophys. Res., 116, doi:10.1029/2009JC005805, 2011.

Cael, B. B. and Follows, M. J.: On the temperature dependence of oceanic export efficiency, Geophys. Res. Lett., 43, 5170-5175, doi:10.1002/2016GL068877, 2016.

Cassar, N., Nevison, C. D., and Manizza, M.: Correcting oceanic O_2/Ar-net community production estimates for vertical mixing using N_2O observations, Geophys. Res. Lett., 41, 8961-8970, doi:10.1002/2014GL062040, 2014.

Cassar, N., Bender, M. L., Barnett, B. A., Fan, S., Moxim, W. J., Levy, H., and Tilbrook, B.: The Southern Ocean biological response to aeolian iron deposition, Science, 317, 1067-1070, doi:10.1126/science.1144602, 2007.

Cassar, N., DiFiore, P. J., Barnett, B. A., Bender, M. L., Bowie, A. R., Tilbrook, B., Petrou, K., Westwood, K. J., Wright, S. W., and Lefevre, D.: The influence of iron and light on net community production in the Subantarctic and Polar Frontal Zones, Biogeosciences, 8, 227-237, doi:10.5194/bg-8-227-2011, 2011.

Craig, H. and Hayward, T.: Oxygen supersaturation in the ocean: Biological versus physical contributions, Science, 235, 199-202, doi:10.1126/science.235.4785.199, 1987.

de Boyer Montegut, C., Madec, G., Fischer, A. S., Lazar, A., and Iudicone, D.: Mixed layer depth over the global ocean: An examination of profile data and a profile-based climatology, Journal of Geophysical Research-Oceans, 109, doi:10.1029/2004JC002378, 2004.

Dong, S., J. Sprintall, Gille, S. T., and Talley, L.: Southern Ocean mixed-layer depth from Argo float profiles, Journal of Geophysical Research-Oceans, 113, doi:10.1029/2006JC004051, 2008.

Eveleth, R., Timmermans, M. L., and Cassar, N.: Physical and biological controls on oxygen saturation variability in the upper Arctic Ocean, Journal of Geophysical Research-Oceans, 119, 7420-7432, doi:10.1002/2014JC009816, 2014.

Eveleth, R., Cassar, N., Sherrell, R. M., Ducklow, H., Meredith, M., Venables, H., Lin, Y., and Li, Z.: Ice melt influence on summertime net community production along the Western Antarctic Peninsula, Deep Sea Research Part II., 139, 89-102, doi:10.1016/j.dsr2.2016.07.016, 2017.

Hamme, R. C., Cassar, N., Lance, V. P., Vaillancourt, R. D., Bender, M. L., Strutton, P. G., Moore, T. S., DeGrandpre, M. D., Sabine, C. L., Ho, D. T., and Hargreaves, B. R.: Dissolved O_2/Ar and other methods reveal rapid changes in productivity during a Lagrangian experiment in the Southern Ocean, Journal of Geophysical Research-Oceans, 117, doi:10.1029/2011JC007046, 2012.

Huang, K., Ducklow, H., Vernet, M., Cassar, N., and Bender, M. L.: Export production and its regulating factors in the West Antarctica Peninsula region of the Southern Ocean, Global Biogeochem Cy, 26, doi:10.1029/2010GB004028, 2012.

Jonsson, B. F., Doney, S. C., Dunne, J. P., and Bender, M. L.: Evaluation of the Southern Ocean O_2/Ar-based NCP estimates in a model framework, Journal of geophysical Research, 118, 385-399, doi:10.1002/jgrg.20032, 2013.

Juranek, L. W., Hamme, R. C., Kaiser, J., Wanninkhof, R., and Quay, P. D.: Evidence of O_2 consumption in underway seawater lines: Implications for air-sea O_2 and CO_2 fluxes, Geophys Res Lett, 37, doi:10.1029/2009GL040423, 2010.

Li, Z. and Cassar, N.: Satellite estimates of net community production based on O_2/Ar observations and comparison to other estimates, Global Biogeochem Cy, 30, 735-752, doi:10.1002/2015GB005314, 2016.

Martin, J. H., Knauer, G. A., Karl, D. M., and Broenkow, W. W.: VERTEX: Carbon Cycling in the Northeast Pacific, Deep Sea Research Part A., 34, 267-285, doi:10.1016/0198-0149(87)90086-0, 1987.

Martin, P., van der Loeff, M. R., Carssar, N., Vandromme, P., d'Ovidio, F., Stemmann, L., Rengarajan, R., Soares, M., González, H. E., Ebersbach, F., Lampitt, R. S., Sanders, R., Barnett, B. A., Smetacek, V., and Naqvi, S. W. A.: Iron fertilization enhanced net community production but not downward particle flux during the Southern Ocean iron fertilization experiment LOHAFEX, Global Biogeochem Cy, 27, 871-881, doi:10.1002/gbc.20077, 2013.

Mouw, C. B., Barnett, A., McKinley, G. A., Gloege, L., and Pilcher, D.: Global ocean particulate organic carbon flux merged with satellite parameters, Earth System Science Data, 8, 531-541, doi:10.5194/essd-8-531-2016, 2016.

Reuer, M. K., Barnett, B. A., Bender, M. L., Falkowski, P. G., and Hendricks, M. B.: New estimates of Southern Ocean biological production rates from O_2/Ar ratios and the triple isotope composition of O_2, Deep Sea Research Part I, 54, 951-974, doi:10.1016/j.dsr.2007.02.007, 2007.

Shadwick, E. H., Tilbrook, B., Cassar, N., Trull, T. W., and Rintoul, S. R.: Summertime physical and biological controls on O_2 and CO_2 in the Australian Sector of the Southern Ocean, J Marine Syst, 147, 21-28, doi:10.1016/j.jmarsys.2013.12.008, 2015.

Stanley, R. H. R., Kirkpatrick, J. B., Cassar, N., Barnett, B. A., and Bender, M. L.: Net community production and gross primary production rates in the western equatorial Pacific, Global Biogeochem Cy, 24, doi:10.1029/2009GB003651, 2010.

Tortell, P. D., Gueguen, C., Long, M. C., Payne, C. D., Lee, P., and DiTullio, G. R.: Spatial variability and temporal dynamics of surface water pCO_2, ΔO_2/Ar and dimethylsulfide in the Ross Sea, Antarctica, Deep Sea Research Part I, 58, 241-259, doi:10.1016/j.dsr.2010.12.006, 2011.

Wanninkhof, R.: Relationship between wind speed and gas exchange over the Ocean, Journal of Geophysical Research-Oceans, 97, 7373-7382, doi:10.1029/92JC00188, 1992.

Werdell, P. J. and Bailey, S. W.: An improved in-situ bio-optical data set for ocean color algorithm development and satellite data product validation, Remote Sensing of Environment, 98, 122-140, doi:10.1016/j.rse.2005.07.001, 2005.